

Data worth and prediction uncertainty for pesticide transport and fate models in Nebraska and Maryland, United States

Bernard T Nolan,^{a*} Robert W Malone,^b John E Doherty,^{c,d} Jack E Barbash,^e Liwang Ma^f and Dale L Shaner^f



Abstract

BACKGROUND: Complex environmental models are frequently extrapolated to overcome data limitations in space and time, but quantifying data worth to such models is rarely attempted. The authors determined which field observations most informed the parameters of agricultural system models applied to field sites in Nebraska (NE) and Maryland (MD), and identified parameters and observations that most influenced prediction uncertainty.

RESULTS: The standard error of regression of the calibrated models was about the same at both NE (0.59) and MD (0.58), and overall reductions in prediction uncertainties of metolachlor and metolachlor ethane sulfonic acid concentrations were 98.0 and 98.6% respectively. Observation data groups reduced the prediction uncertainty by 55–90% at NE and by 28–96% at MD. Soil hydraulic parameters were well informed by the observed data at both sites, but pesticide and macropore properties had comparatively larger contributions after model calibration.

CONCLUSIONS: Although the observed data were sparse, they substantially reduced prediction uncertainty in unsampled regions of pesticide breakthrough curves. Nitrate evidently functioned as a surrogate for soil hydraulic data in well-drained loam soils conducive to conservative transport of nitrogen. Pesticide properties and macropore parameters could most benefit from improved characterization further to reduce model misfit and prediction uncertainty.

Published 2014. This article is a U.S. Government work and is in the public domain in the USA.

Supporting information may be found in the online version of this article.

Keywords: degradates; metolachlor; parameter estimation; prediction uncertainty; RZWQM

1 INTRODUCTION

Studies by the US Geological Survey's National Water Quality Assessment (NAWQA) program have shown that the herbicide metolachlor [2-chloro-*N*-(2-ethyl-6-methylphenyl)-*N*-(2-methoxy-1-methylethyl)acetamide] is among the top four most frequently detected pesticides in groundwater. In a national study, metolachlor was detected in 18% of groundwater samples in agricultural areas, about the same rate as simazine and behind only atrazine and deethylatrazine.¹ The latter two compounds were detected in 42 and 43%, respectively, of groundwater samples in agricultural areas.

It is well known that pesticide occurrence in groundwater is related to application rates, pesticide properties, soil conditions and other factors. Less well known are the processes controlling the transport and fate of degradates, although degradates are frequently detected in the nation's water resources. Nationwide, one or more pesticides or degradates were detected 61% of the time in shallow groundwater beneath agricultural areas.¹ Additionally, NAWQA studies in eastern Iowa showed that nearly 85% of the total mass of herbicide in stream samples comprised ten degradates (including metolachlor degradates), and that the summed concentration of degradates was more than 10 times higher than that of the parent compounds.

Few studies have attempted to simulate transport of both applied pesticides and their degradates in multiple agricultural settings of the United States. Here, use was made of inverse modeling at field sites in Nebraska (NE) and Maryland (MD) (Fig. 1) to calibrate the Root Zone Water Quality Model (RZWQM)² for predicting the transport and fate of metolachlor, metolachlor ethane sulfonic acid [2-[(2-ethyl-6-methylphenyl)(2-methoxy-1-methylethyl)amino]-2-oxoethanesulfonic acid] (ESA) and metolachlor oxanilic acid [2-[(2-ethyl-6-methylphenyl)

* Correspondence to: Bernard T Nolan, US Geological Survey, 413 National Center, Reston, VA 20192, USA. E-mail: btnolan@usgs.gov

a US Geological Survey, Reston, VA, USA

b US Department of Agriculture, Ames, IA, USA

c Watermark Numerical Computing, Corinda, Australia

d National Centre for Groundwater Research and Training, Flinders University, Australia

e US Geological Survey, Tacoma, WA, USA

f US Department of Agriculture, Fort Collins, CO, USA

EXPLANATION

- A. Central Nebraska Basins
Maple Creek Study Basin
- B. Potomac River Basin and
Delmarva Peninsula
Morgan Creek Study Basin

- N23
○ Monitoring well site and I.D.
- ★ Unsaturated zone monitoring site

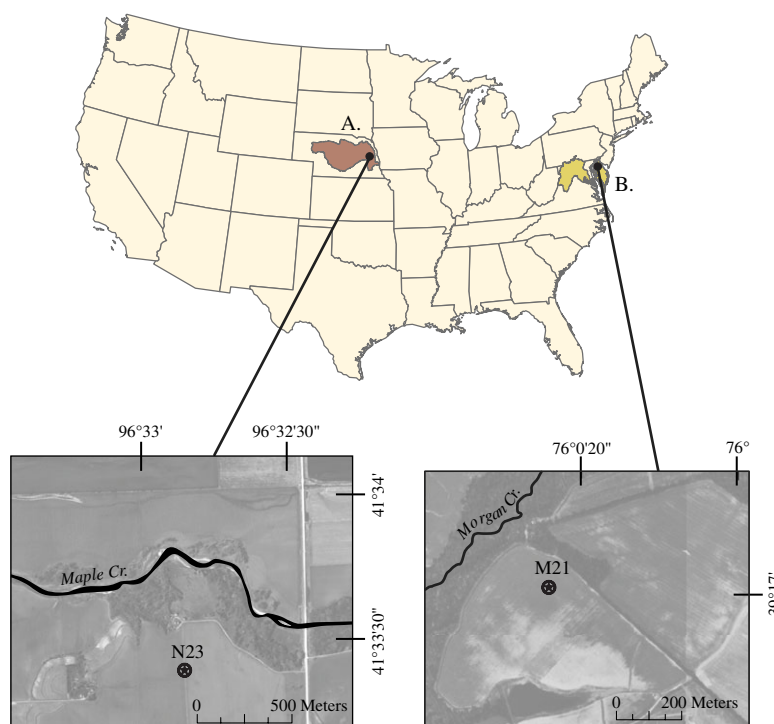


Figure 1. Site map showing unsaturated zone monitoring locations in Nebraska and Maryland

(2-methoxy-1-methylethyl)amino]-2-oxoacetic acid} (OXA). The calibrations used pesticide data, nitrate data and, at MD, observations of soil moisture and soil water tension. Nitrate transport was simulated by the RZWQM nitrogen module using parameters obtained during previous inverse modeling at these same sites.³ Conservative transport of nitrate was expected on the basis of previous results, so it was anticipated that nitrate would function primarily as a tracer.

Inverse modeling was conducted in tandem with analyses of data worth and prediction uncertainty. Among the many reasons for modeling an environmental system, perhaps the main reason is to overcome the limitations of field observations in space and time.⁴ Models are tools by which to extrapolate from available observations to gain a greater understanding of the system. Additionally, field observations are costly to obtain and may be scarce. In the present study, the MD pesticide data comprised 7 months of sampling and represented only the tail of the breakthrough curve (BTC); soil hydraulic data were not sampled at NE; all data at both sites were collected from working farms, which limited access to fields at certain times.

To address concerns with model extrapolation and data adequacy, in this field example, data worth and prediction uncertainty are emphasized over traditional measures of model fit. The linear equations used here do not require a model to employ parameters that provide a good fit with field data, as they are applicable in a generic sense. Linear sensitivity and uncertainty metrics can help users to identify which parameters are well informed by the data, which parameters are important to the predictions and which observations are most instrumental in reducing the uncertainties of predictions of interest. In their capacity to identify parameters that contribute most to the uncertainties of key predictions, and to quantify the effectiveness of different data acquisition strategies in reducing these contributions, linear methods are more efficient

than global uncertainty analyses based, for example, on methodologies such as Markov-chain Monte Carlo.^{5–8} While the latter method provides a full implementation of the Bayes equation, quantification of posterior predictive uncertainty requires many model runs. The number of these runs is greatly increased where an analysis then attempts to quantify increases or reductions in parameter and predictive uncertainty following reduction and expansion of the number and nature of field observations. In contrast, the numerical burden of linear uncertainty analysis and ancillary linear analyses in which data worth and parameter contributions to predictive uncertainty are assessed is very small. A disadvantage of linear methods is their approximate nature. However, this disadvantage must be seen in context, particularly where alternative non-linear analysis may be impossible owing to the very large number of model runs required. Added to this is the fact that even non-linear methods require approximations to be made, one such approximation being the adoption of a covariance matrix to quantify measurement noise where, in fact, most contributions to model-to-measurement misfit are the outcomes of model-based structural noise whose covariance matrix is unknown, and most probably singular.⁹

Linear methods have been compared with Markov-chain Monte Carlo and found to produce similar results. Heuristic tests of analytical and numerical models in a prior study suggested that linear confidence intervals were useful approximations of uncertainty even when conditions of Gaussian errors and small intrinsic non-linearity were significantly violated.¹⁰ In another study, researchers analyzed the performance of linear methods when used in conjunction with highly non-linear models.¹¹ They showed that, while the exact outcomes of linear analysis may indeed depend on local parameter values, these outcomes are likely to be qualitatively robust in that ordering relationships determined for parameter contributions to predictive uncertainty and the worth

Table 1. General characteristics of the two field sites

Site	Mean precipitation (cm year ⁻¹)	Irrigation rate (cm year ⁻¹)	Depth to water ^a (m)	Soil type	Pesticide application
Nebraska (N23): corn–soybean (Dodge County)	72	20	21.6	Loam	Metolachlor, 0.67 kg ha ⁻¹ , 9 May 2002 and 2004
Maryland (M21): corn–soybean (Kent County)	112	0	≥6.50	Sandy loam	Metolachlor, 1.36 kg ha ⁻¹ , 20 April 2002

^a At monitoring well during model simulation period; water level in Maryland decreased during the simulation period.

of different types of data are relatively invariant as parameter values are changed.

Calibration of agricultural system models is required under most circumstances, and estimating the value of the available data for this type of modeling is essential. Knowing the most important parameters and which among the available observations inform those parameters can help users to focus sampling and modeling resources to where they are most needed. However, quantifying data worth to model calibration is rare in pesticide modeling research. Accordingly, the objectives in the present field example were: (1) to identify sensitive model parameters; (2) to determine which observations most informed the parameters; (3) to identify which parameters and observation groups most influenced prediction uncertainty for unsampled portions of the BTCs.

2 METHODS

2.1 Field sites and data collection

The general characteristics of the field sites are shown in Table 1. Previous investigators¹² used RZWQM to predict metolachlor transport and fate at the MD site. Aspects of the present study that differed from the previous work included: (1) use of inverse modeling for parameter estimation and sensitivity and uncertainty analyses; (2) expansion of the pesticide modeling to an additional site (NE); (3) at MD, inclusion of pesticide data from two deeper lysimeters (1.3 and 2.4 m), whereas Bayless *et al.*¹² manually calibrated RZWQM to data from the shallowest (0.5 m) lysimeter; (4) estimation and evaluation of macropore parameters at both sites. The previous modeling studies^{3,12} did not use the RZWQM macropore component. Here, inverse modeling was used to estimate macropore parameters in a consistent way at both sites. Therefore, an additional aspect of the study was evaluation of the influence of macropores at the two sites on the basis of the inverse calibrated models.

Briefly, the sites comprised N23, an irrigated corn–soybean rotation in the Maple Creek study basin in eastern NE, and M21, a corn–soybean rotation in the Morgan Creek study basin in eastern MD (Fig. 1). Both sites were described in previous studies,^{3,13,14} and the sampling of pesticides, degradates, nitrate and bromide was described by Capel *et al.*¹³ A brief description of site activities follows. The NE site received 0.67 kg ha⁻¹ of metolachlor in 2002 and 2004, and 1.36 kg ha⁻¹ of metolachlor was applied at MD in 2002 (Table 1). Pesticide and degradate samples were collected from April 2004 to June 2005 in NE and from March to September 2004 in MD. Thus, at MD nearly 2 years had elapsed since metolachlor was applied; however, lysimeter sampling at MD consistently yielded detectable levels of ESA and OXA. NE had more complete pesticide data than MD; lysimeter sampling spanned the BTCs, although there is no metolachlor observation corresponding to

Table 2. Observation groups and weights used in model calibration by PEST parameter estimation software

Observation	Number	Range	Weight used with PEST
Nebraska			
Metolachlor (mg L ⁻¹)	27	0.000013–0.0017	1500
Metolachlor ethane sulfonic acid (mg L ⁻¹)	23	0.00013–0.019	190
Metolachlor oxanilic acid (mg L ⁻¹)	23	0.00024–0.013	251
Nitrate (mg L ⁻¹)	43	4.5–58.8	0.03
Maryland			
Metolachlor (mg L ⁻¹) ^a	14	ND ^b	10 000
Metolachlor ethane sulfonic acid (mg L ⁻¹)	14	0.00024–0.0019	2500
Metolachlor oxanilic acid (mg L ⁻¹)	14	0.00015–0.00082	7500
Nitrate (mg L ⁻¹)	34	3.0–50.5	0.03
Soil moisture content (cm ³ cm ⁻³)	204	0.12–0.28	10
Soil water tension (cm)	204	–5800–0	0.001

^a Metolachlor, the parent compound, was not detected in any of the lysimeter samples; metolachlor reporting level = 0.00001 mg L⁻¹.
^b ND: not detected.

the predicted peak concentration. All 73 metolachlor and degradate concentrations at NE were above the reporting level (Table 2). Lysimeters that had detectable concentrations of pesticides were located at depths of 1.5 and 7.0 m at NE and 0.5, 1.3 and 2.4 m at MD.¹³

Soil moisture and soil water tension are directly related to water retention functions used by RZWQM to compute water fluxes, and were extensively sampled at MD. Collection of such data spanned 15 months and represented a complete wetting and drying cycle, including comparatively dry conditions in September 2004. Soil moisture was measured at MD by water content reflectometry probes located at depths of 0.5, 0.8, 1.1 and 1.4 m, and soil water tension was measured by heat dissipation probes located at depths of 0.4, 1.1, 2.3 and 4.1 m.¹³ Soil hydraulic data were not collected at NE.

Soil samples from Iowa State University's Northeast Research Center near Nashua, Iowa, were analyzed to determine the partition coefficients (K_d) of metolachlor and OXA as part of a follow-up modeling study for a site in Iowa. Because soil samples were no longer available at NE and MD, the Iowa K_d values were compared with those at NE and MD derived through model calibration. Measured organic matter content at NE and MD was considered

when making the K_d comparisons. The eight soil samples at lowa were collected from two 0.4 ha field plots comprising moderately well to poorly drained loam and silty clay-loam soils.¹⁵ K_d was measured for each soil sample using methods described in the supporting information.

2.2 Unsaturated zone fate and transport modeling

Version 2.4 of RZWQM was used to simulate pesticide transport and fate and water fluxes at the two field sites. RZWQM is a one-dimensional agricultural system model that simulates the effects of agricultural management practices on soils, crop growth and water quality.^{2,16} RZWQM simulates water and pesticide movement in the soil matrix, overland flow and macropore flow. The latter two pathways have the potential to transfer pesticides more quickly compared with soil matrix flow. RZWQM simulates soil infiltration of water on the basis of the Green-Ampt equation, and water is redistributed within the soil according to the Richards' equation.¹⁷ When rainfall and/or irrigation exceed the infiltration rate of the soil, a portion of chemicals in the top 2 cm of soil ('mixing zone') can be transferred to overland flow where they can either enter macropores or become edge-of-field run-off, depending on macropore flow capacity. Solution moving through macropores interacts with soil walls, and a portion of the water and chemicals infiltrates outwards into the soil matrix. The interaction with macropore walls is simulated with a parameter describing effective soil thickness (est), which is the thickness of a macropore wall available for interaction with water and chemicals.¹⁸ Radial flow outwards from macropores into the soil matrix can be impeded by compaction of the macropore walls, and this effect is simulated using the sorptivity factor control for lateral infiltration (lsf). Most percolate comes from a small number of macropores, and this is addressed through the concept of 'active macroporosity'. The active macroporosity is the fraction of total macroporosity that transmits water, and is a function of the number of macropores per unit area that effectively transmit water.¹⁹ Active macroporosity was calculated as one-half of the percolate-producing macroporosity according to

$$p_{mac} = 0.5 \times n_{mac} \times \pi \times rad^2 \quad (1)$$

where p_{mac} is active macroporosity, n_{mac} is the number of percolate-producing macropores per soil area (cm^{-2}) and rad is the average radius of macropores (cm).¹⁸ The n_{mac} parameter was adjusted during inverse modeling, and p_{mac} was calculated externally by a post-processor.

RZWQM simulates pesticide sorption, desorption and degradation, and the latter is simulated as a first-order process. Sorption is characterized by K_d , which is normalized to soil organic carbon according to $K_{oc} = K_d/f_{oc}$, where K_{oc} is the soil organic carbon sorption coefficient and f_{oc} is the weight fraction of organic carbon in the soil. In the present study, RZWQM was parameterized for simultaneous degradation of metolachlor to the degradates ESA and OXA. Pesticide half-life is influenced by soil water content and temperature, and these effects are simulated in RZWQM from the predicted field temperature and water content of the soil, reference soil temperature and soil water content, activation energy and other parameters.¹⁹

Model set-up for nitrate has been previously described,³ but here the MD model was extended nearly to the average water table depth (6.54 m) to account for macropore flow of water and pesticides to depth. Measured depth to water decreased during the period of data collection at MD, so a unit gradient boundary

condition was used rather than constant head. Initial tests established that both boundary conditions gave identical results at the depth of data collection (0.5–4.1 m). The model simulation periods were 2002–2004 at MD and 2002–2005 at NE. The RZWQM simulation iteration control was used to run the model a second time after reading state values from the end of the first simulation. This doubled the simulation periods, helped to stabilize hydraulic properties and nutrient pools and allowed for residual pesticide concentrations in soil and water. Simulation layers associated with each model are shown in supporting information Table S1.

PEST²⁰ was used to estimate parameters pertaining to the soil water, pesticide and macropore components of RZWQM. PEST uses a combination of singular value decomposition supported by Tikhonov regularization as a basis for parameter estimation. Although 'gradient methods' implemented by PEST have the potential to become trapped in local objective function minima, here several sets of starting parameters were used, and these converged on similar parameter values. PEST attempts model calibration through near-minimization of a weighted least-squares objective function, given by the equation

$$\Phi(\mathbf{b}) = \sum_{i=1}^{m_1} \omega_{sm,i}^2 (O_{sm,i} - P_{sm,i})^2 + \sum_{i=1}^{m_2} \omega_{t,i}^2 (O_{t,i} - P_{t,i})^2 + \sum_{i=1}^{m_3} \omega_{n,i}^2 (O_{n,i} - P_{n,i})^2 + \sum_{i=1}^{m_4} \omega_{mt,i}^2 (O_{mt,i} - P_{mt,i})^2 + \sum_{i=1}^{m_5} \omega_{e,i}^2 (O_{e,i} - P_{e,i})^2 + \sum_{i=1}^{m_6} \omega_{o,i}^2 (O_{o,i} - P_{o,i})^2 + \Phi\mathbf{M} \quad (2)$$

where $\Phi(\mathbf{b})$ is the measurement objective function based on parameter set (\mathbf{b}) , P is the predicted value, O is the observed value, ω is the observation weight, subscript i denotes the i th observation, subscript 'sm' denotes soil moisture, subscript 't' denotes soil water tension, subscript 'n' denotes nitrate, subscript 'mt' denotes metolachlor, subscript 'e' denotes ESA, subscript 'o' denotes OXA, m_1, m_2, \dots, m_6 are the numbers of observations associated with each of the preceding observation groups and

$$\Phi\mathbf{M} = \sum \omega_{ij} (p_{ej} - p_j)$$

where estimated parameter values (p_j) are penalized as part of Tikhonov regularization in proportion to their departures from expert-knowledge-based values (p_{ej}), and the regularization weights ω_{ij} are adjusted by PEST in accordance with the user's desire for the measurement objective function to attain a certain level, discussed below. All observation groups were used as part of a multi-objective optimization approach, which can mitigate parameter equifinality wherein multiple sets of parameters lead to acceptable model results.²¹ Additionally, prior researchers found that multi-objective optimization reduced model uncertainty compared with extending the period of data collection or sampling frequency of a single observation group.²² At NE, equation (2) excluded the first two terms because soil moisture and water tension data were not collected.

Tikhonov regularization commonly results in a value of $\Phi(\mathbf{b})$ that is somewhat greater than the lowest obtained from an initial, non-regularized optimization (see below). The former is set by the PEST variables PHIMLIM, which controls the strength of regularization, and PHIMACCEPT, which helps account for deviations from linearity that can arise from linear approximation of the equations

used to derive the parameter estimates.²³ Less regularization improves the model fit but can result in parameters reaching their bounds, whereas greater regularization sacrifices model fit to some degree but can yield more realistic parameter estimates. After regularization, $\Phi(\mathbf{b})$ typically is commensurate with levels of so-called 'structural noise' which is an outcome of a model's inability to simulate the totality of all processes that are operative at a particular site. This is often heuristically determined from the level of fit at which parameter values indicate that parameters are playing compensatory roles in order to accommodate model defects.

Observation groups, related statistics and corresponding weights are shown in Table 2. The weighting strategy was twofold: (1) to compensate for extreme differences in units (e.g. 10^{-4} mg L⁻¹ pesticide concentrations versus 10^4 cm soil water tensions); (2) to ensure that no single observation group dominated or was dominated by any other group in $\Phi(\mathbf{b})$, thereby ensuring that the information content of each observation group was allowed access to the parameter estimation process, and could thereby influence the estimated values of parameters. Regarding the latter, the weights were initially set as the inverse of the variance of the observation error, as recommended by prior researchers.⁷ The weights were then adjusted to emphasize pesticide and degradate concentrations relative to the other observation groups. This step was intended to account for epistemic uncertainty, which includes measurement error, model error and structural/conceptual uncertainty.²⁴

Parameter estimation was conducted in two phases. Firstly, PEST was used to lower the measurement objective function to as low a level as could be achieved with the calibration data ($\Phi\mathbf{M}=0$). During calibration, truncated singular value decomposition was used to estimate linear combinations of process-model parameters, which mitigated problems with parameter correlation and insensitivity. The second phase utilized regularization, whereby the target objective function was set 5–10% higher than the minimum and the process was repeated. This procedure ensured that the fit between model outputs and field data was near optimal while providing more realistic values of estimated parameters. See the PEST documentation for further implementation details.^{20,25}

Following parameter estimation, predictive uncertainty analysis was performed using linear methods. This step required calculation of a sensitivity matrix on the basis of the estimated parameters; this matrix lists the sensitivity of every model output used in the calibration process to every parameter. Linear analysis also required that a prior parameter covariance matrix be provided. As the covariance matrix associated with the prior probability distribution of parameters, this can be viewed as an expression of expert knowledge (or a lack thereof, as it pertains to parameter values at any particular study site). The inherent parameter variability is used in an informal Bayesian approach which is described in more detail below.

2.3 Model fit, sensitivity and prediction uncertainty

The index of agreement (IA) was used to describe the degree of fit of the calibrated models, defined as²⁶

$$IA = 1 - \frac{\sum_{i=1}^m (O_i - P_i)^2}{\sum_{i=1}^m (|P_i - \bar{O}| + |O_i - \bar{O}|)^2} \quad (3)$$

where \bar{O} is the mean of the observations, and m is the number of observations. The index of agreement ranges from 0 to 1, with higher values indicating better fit.²⁶

PEST's SUPOBSPAR1 utility²⁵ was used to track the flow of information from combinations of observations to combinations of parameters obtained by undertaking singular value decomposition on the weighted sensitivity matrix. SUPOBSPAR1 defines so-called 'superobservations' (linear combinations or eigenvectors of individual observations) that directly and entirely inform so-called 'superparameters' (eigenvectors of process-model parameters). In the parameter estimation process, each superparameter (SP) can be shown to be calculable from its corresponding superobservation (SO) through direct multiplication of the latter by the singular value with which both are associated. Individual observations with activities of more than about 0.1 on the SO eigenvectors were considered most to inform the corresponding SPs. Squaring and summing the activities of the process-model parameters for eight of the SPs estimated here yielded the parameter identifiability statistic (ID),⁶ which indicates the amount of information provided by the observed data for estimating a parameter (i.e. parameter sensitivity).

PEST's GENLINPRED utility was used to perform predictive uncertainty analysis based on a linearized Bayesian approach that computes predictive uncertainty variance as^{24,25}

$$\sigma_s^2 = \mathbf{z}^T \mathbf{C}_{pp} \mathbf{z} - \mathbf{z}^T \mathbf{C}_{pp} \mathbf{X}^T [\mathbf{X} \mathbf{C}_{pp} \mathbf{X}^T + \mathbf{C}_{\epsilon\epsilon}]^{-1} \mathbf{X} \mathbf{C}_{pp} \mathbf{z} \quad (4)$$

where σ_s^2 is the posterior uncertainty of the single prediction, \mathbf{z} is a vector of prediction sensitivities, \mathbf{X} is the sensitivity (sometimes called 'Jacobian') matrix comprising m rows and n columns, where m is the number of observations with non-zero weights and n is the number of parameters, \mathbf{C}_{pp} is the covariance matrix of the prior parameter variability with variances on the diagonal and covariances on the off-diagonal and $\mathbf{C}_{\epsilon\epsilon}$ is the covariance matrix of simulation error and measurement error (which, as is usually done, are lumped together in a single matrix that reflects model-to-observation misfit). The first term in equation (4) represents precalibration (*a priori*) predictive uncertainty, and the second term represents the reduction in prior uncertainty incurred by the conditioning effect of the calibration dataset.²⁴ \mathbf{C}_{pp} was based on statistical distributions of parameters to the extent possible. For example, standard deviations of soil hydraulic properties were included in the parameter uncertainty file used by GENLINPRED. Prior researchers compiled generic distributions of soil hydraulic parameters and compared them with parameter values from other sources.²⁷ The most significant differences occurred for a curve-fitting parameter related to the pore size distribution in the Brooks–Corey water retention function, but that parameter was not directly estimated in the present study.

GENLINPRED accesses several PEST utilities, which are briefly described here. PREDUNC1^{25,28} was used to compute the precalibration uncertainty of the predictions, and to derive postcalibration prediction intervals for deep seepage to evaluate the water component of RZWQM. Parameter contributions to the uncertainty of predicted maximum pesticide or degradate concentration were evaluated using PREDUNC4,^{24,25,28} which computes pre- and postcalibration components of σ_s^2 before and after perfect knowledge of a parameter is assumed (this being indicated mathematically by setting pertinent rows/columns of \mathbf{C}_{pp} to zero). The resulting reductions in the pre- and postcalibration components of prediction uncertainty represent the contribution of the parameter to the prediction uncertainty. Stated loosely, the greater the

reduction in predictive uncertainty, the greater is the importance for that parameter to the prediction, denoted as 'parameter importance' (PI) herein.

PREDUNC5^{24,25,28} was used to compute data worth for groups of observations (metolachlor, ESA, OXA, etc.). PREDUNC5 provides two metrics: (1) the decrease in precalibration predictive uncertainty variance [first term in equation (4)] that is accrued if the observation or observation group comprises the entirety of the calibration dataset; (2) the increase in predictive uncertainty variance [both terms in equation (4)] incurred through omission of the observation group from the calibration dataset (simulated by adding rows to and removing rows from the \mathbf{X} matrix). The first quantity is a measure of the information content of the observation group with respect to each prediction; the second is a measure of the uniqueness of that information. In the discussion that follows, all changes to predictive uncertainty variance were normalized through division by the total precalibration predictive uncertainty variance and expressed as percentages to facilitate comparison between locations and between predictions.

As stated above, equation (4) was employed for computation of predictive uncertainty variance, and for changes in predictive uncertainty variance following the assumption of perfect knowledge of parameters and by addition/removal of selected observations to/from the calibration dataset. The \mathbf{C}_{pp} matrix, as discussed above, is a reflection of expert knowledge. This was supplied as a diagonal matrix whose diagonal terms are the squares of prior parameter uncertainty standard deviations. \mathbf{C}_{ee} is a diagonal matrix comprising values calculated from the components of the objective function acquired through the model calibration. Elements of this matrix were set in such a way that the components of $\Phi(\mathbf{b})$ corresponding to each observation group equaled the number of observations comprising the group. In this way, both the measurement and model errors that give rise to model-to-observation misfit were in harmony with assessments of misfit made through the calibration process.

3 RESULTS AND DISCUSSION

3.1 Model fit to observed data

Inverse modeling calibration resulted in 289 RZWQM simulations at NE and 447 simulations at MD. The standard error of regression [see supporting information equation (S1)] of the calibrated models was about the same at NE (0.59) and MD (0.58), indicating that both models provided about the same overall fit to the data. The hydrology component of the MD model fitted the observed soil hydraulic data well: IA = 0.90 for soil moisture data and IA = 0.95 for soil water tension data.

Predicted concentrations of metolachlor and degradates fitted the observed data reasonably well at NE (Fig. 2): IA was 0.68 for metolachlor, 0.81 for ESA and 0.85 for OXA. The period of data collection at NE spanned the breakthrough and recession of metolachlor and degradates such that these compounds varied in a systematic way over time (Fig. 2). RZWQM predicted fairly rapid appearance of metolachlor and degradates in late May 2004, followed by declining concentrations the following summer, although there were gaps in the measured data in late May–June 2004 (corresponding to predicted peak concentrations) and from October 2004 to April 2005 (Fig. 2). The rise and fall of measured and predicted values apparently benefitted the IA statistic, which is a correlative measure.

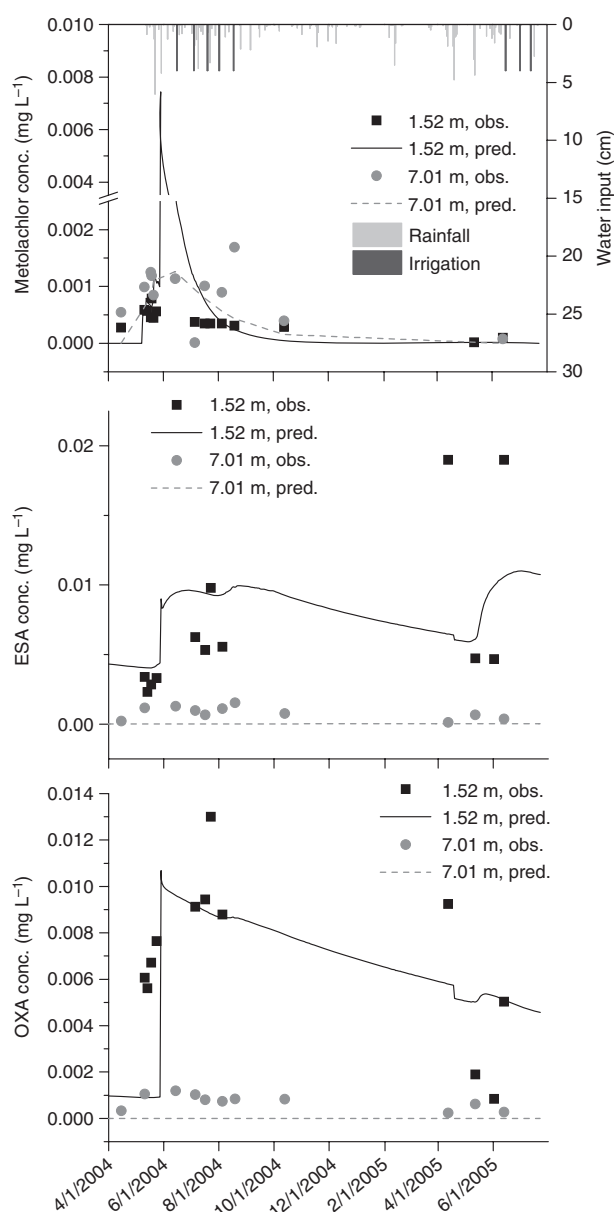


Figure 2. Predicted versus observed concentrations of metolachlor, metolachlor ethane sulfonic acid (ESA) and metolachlor oxanilic acid (OXA) over time in Nebraska. Water inputs from precipitation and irrigation are shown in the top plot.

Pesticide data were more sparse at MD than at NE. Lysimeter samples were procured 2 years after metolachlor was applied on 20 April 2002, and the observed data (March–September 2004) characterized only the tail of the BTC (Fig. 3). Additionally, all 14 metolachlor observations at MD were less than the reporting level of 10^{-5} mg L⁻¹ in 2004 (Table 2). The metolachlor non-detects were still useful in model calibration, however, and corresponding metolachlor predictions were all below 10^{-6} mg L⁻¹, indicating reasonable agreement (data not shown). IA values of ESA (0.42) and OXA (0.30) at MD were substantially lower than at NE, indicating comparatively poor fit to the degradate data. In contrast to NE, measured and predicted degradate values at MD were relatively constant over time (Fig. 3).

Figure 4 shows that the poor fit of the model at MD was confined to the shallow lysimeter (0.5 m). Measured and predicted

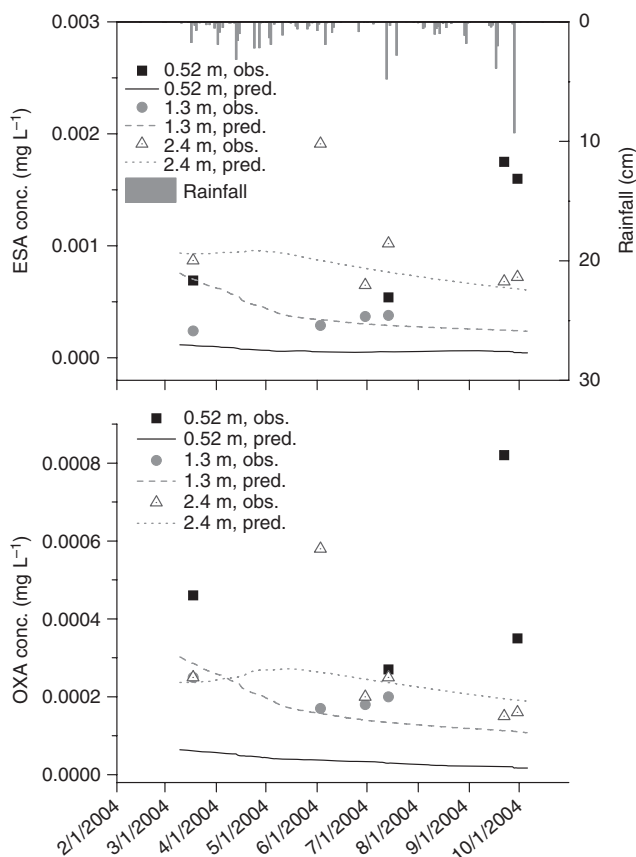


Figure 3. Predicted versus observed concentrations of metolachlor ethane sulfonic acid (ESA) and metolachlor oxanilic acid (OXA) over time in Maryland. Water input from precipitation is shown in the top plot.

concentrations corresponding to the deeper lysimeters were well within a factor of 5 for both ESA and OXA. In a paper on simulated atrazine transport in drainage, predicted concentrations in the soil profile within a factor of 10 of measured concentrations were considered to be acceptable, and predicted concentrations in drainage within a factor of 5 of measured were considered very good.²⁹ In the present study, 71% of predicted ESA and OXA values were within a factor of 5 of measured values, and 79% of predicted ESA values and 86% of predicted OXA values were within a factor of 10.

Although RZWQM underestimated degradate concentrations at 0.5 m at MD, the predicted depletion of degradates at shallow depth is reasonable because of the elapsed time since metolachlor application. The observed persistence of degradates at this depth may be due to processes not simulated here. For example, we did not estimate RZWQM parameters associated with sorption kinetics. However, kinetic and equilibrium-only approaches produced similar results in a previous pesticide modeling study.²⁹

Prior researchers discussed potential sequestration of atrazine on surficial woody debris in fine-grain material at MD site M22,¹⁴ which is adjacent to the modeling site in the present study. Solids concentrations of both atrazine and deethylatrazine (DEA) were high at shallow depth (<2 m) 2 years after the last atrazine application in 2002, while corresponding water samples contained DEA but not atrazine. Similarly, sequestration of metolachlor on woody solids might have provided a source of degradate to soil water at shallow depth long after this compound was applied.

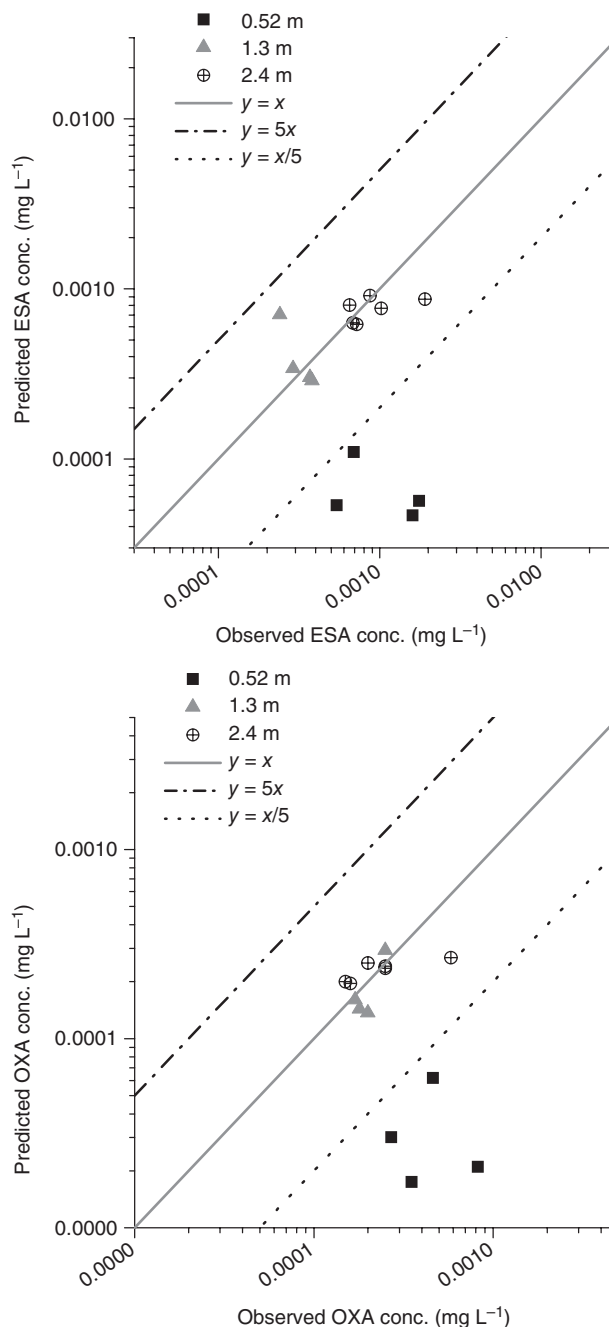


Figure 4. Predicted versus observed concentrations of metolachlor ethane sulfonic acid (ESA) and metolachlor oxanilic acid (OXA) in Maryland in relation to lines representing predicted concentrations within a factor of 5 of observed concentrations.

3.2 Model parameter estimates

Parameter estimates and ID values obtained by inverse modeling are shown in Table 3. Estimates of soil hydraulic parameters generally were consistent with previous models that emphasized N mass balances at these sites.³ Here, pesticide and degradate parameters are emphasized, in keeping with the present objectives. PEST-calibrated values of K_{oc} and half-life were mostly consistent with ranges reported in the literature, although differences arose in cases where f_{oc} and temperature were different from field conditions at NE and MD. Pesticide properties are discussed in more detail in the supporting information. However, results should

Table 3. Root Zone Water Quality Model parameters obtained by inverse modeling in Nebraska and Maryland and identifiability values based on all of the observations [L1 to L5, modeled soil layers comprising lm (loam), snd (sand), stlm (silt loam), sdllm (sandy loam); ID, identifiability; ESA, metolachlor ethane sulfonic acid; OXA, metolachlor oxanilic acid]

Name	Nebraska		Maryland		
	Estimate	ID	Estimate	ID	
Hydraulic properties					
Saturated hydraulic conductivity (cm hr^{-1}) for each modeled soil layer					
L1 ^a NE sdllm; MD: lm	ks1	5.90	0.002	0.11	0.117
L2 ^a NE sdllm; MD: lm	ks2	19.39	0.008	1.08	0.087
L3 ^a NE stlm; MD: sdllm	ks3	5.29	0.002	5.62	0.209
L4 ^a NE snd; MD: lm	ks4	16.71	0.009	1.91	0.064
L5 ^a NE snd; MD: sdllm	ks5	13.83	0.004	5.27	0.115
Water content at field capacity ($\text{cm}^3 \text{cm}^{-3}$) for each modeled soil layer					
L1 ^a (all soil layers same as above)	wfc1	0.12	0.687	0.25	0.268
L2 ^a	wfc2	0.14	0.693	0.16	0.505
L3 ^a	wfc3	0.28	0.116	0.11	0.627
L4 ^a	wfc4	0.13	0.022	0.21	0.004
L5 ^a	wfc5	0.22	0.004	0.15	0.007
Bulk density (g cm^{-3}) for each modeled soil layer					
L1 ^a (all soil layers same as above)	bd1	1.47	2.584	1.70	2.279
L2 ^a	bd2	1.66	2.640	1.69	1.789
L3 ^a	bd3	1.55	0.005	1.70	1.073
L4 ^a	bd4	1.70	0.246	1.21	0.114
L5 ^a	bd5	1.70	0.011	1.20	0.179
Pesticide properties					
Sorption coefficient ($\text{cm}^3 \text{g}^{-1}$), metolachlor	koc1	187.10	0.040	375.00	0.055
Sorption coefficient ($\text{cm}^3 \text{g}^{-1}$), ESA	koc2	74.93	0.093	24.92	6.86E-05
Sorption coefficient ($\text{cm}^3 \text{g}^{-1}$), OXA	koc3	13.59	0.001	27.01	2.46E-05
Formation %, ESA	for1	49.97	0.060	18.55	8.56E-06
Formation %, OXA	for2	70.00	0.044	43.45	2.20E-05
Soil surface biotic half-life (days), metolachlor	tsb	5.00	0.012	23.66	3.88E-05
Soil subsurface aerobic half-life (days), metolachlor	tsba	7.56	0.071	17.14	0.084
Soil subsurface aerobic half-life (days), ESA	td1a	166.08	0.314	115.78	2.61E-05
Soil subsurface aerobic half-life (days), OXA	td2a	200.00	0.007	106.76	5.93E-05
Macropore parameters					
Crust hydraulic conductivity (cm h^{-1})	chc	0.01	0.025	0.050	6.73E-53
Fraction microporosity	fmic	0.52	0.003	0.50	0.040
Effective soil thickness (cm)	est	0.097	0.088	0.71	0.180
Sorptivity factor control for lateral infiltration (cm)	lsf	0.0016	0.026	0.048	0.035
Number of macropores per cm^2	nmac	0.033	0.128	0.030	0.018
Average macropore radius (cm)	rad	0.063	0.053	0.049	0.152

^a Depth intervals (cm) of the five model layers at each site were: Nebraska 0–10, 10–244, 244–366, 366–732, 732–1000; Maryland 0–10, 10–100, 100–250, 250–400, 400–648.

be interpreted with caution because the BTCs were undersampled at both sites.

The calibrated values of K_{oc} and half-life for metolachlor, ESA and OXA differed between NE and MD (Table 3), but the overall relations were consistent. Firstly, K_{oc} was substantially lower for both degradates ($14\text{--}75 \text{ cm}^3 \text{ g}^{-1}$) than for metolachlor ($187\text{--}375 \text{ cm}^3 \text{ g}^{-1}$) at both sites, indicating greater water solubility and increased mobility of the degradates relative to the parent

compound. Secondly, half-lives were substantially greater for the two degradates (107–200 days) than for metolachlor (5–24 days) at both sites, indicating greater persistence. This is consistent with patterns of occurrence of the three compounds in the subsurface; several studies have reported substantially higher frequencies of detection for the two degradates than for metolachlor in groundwater,^{30–32} as well as in surface water under base flow conditions.³³ Thirdly, differences in calibrated K_{oc} values at NE

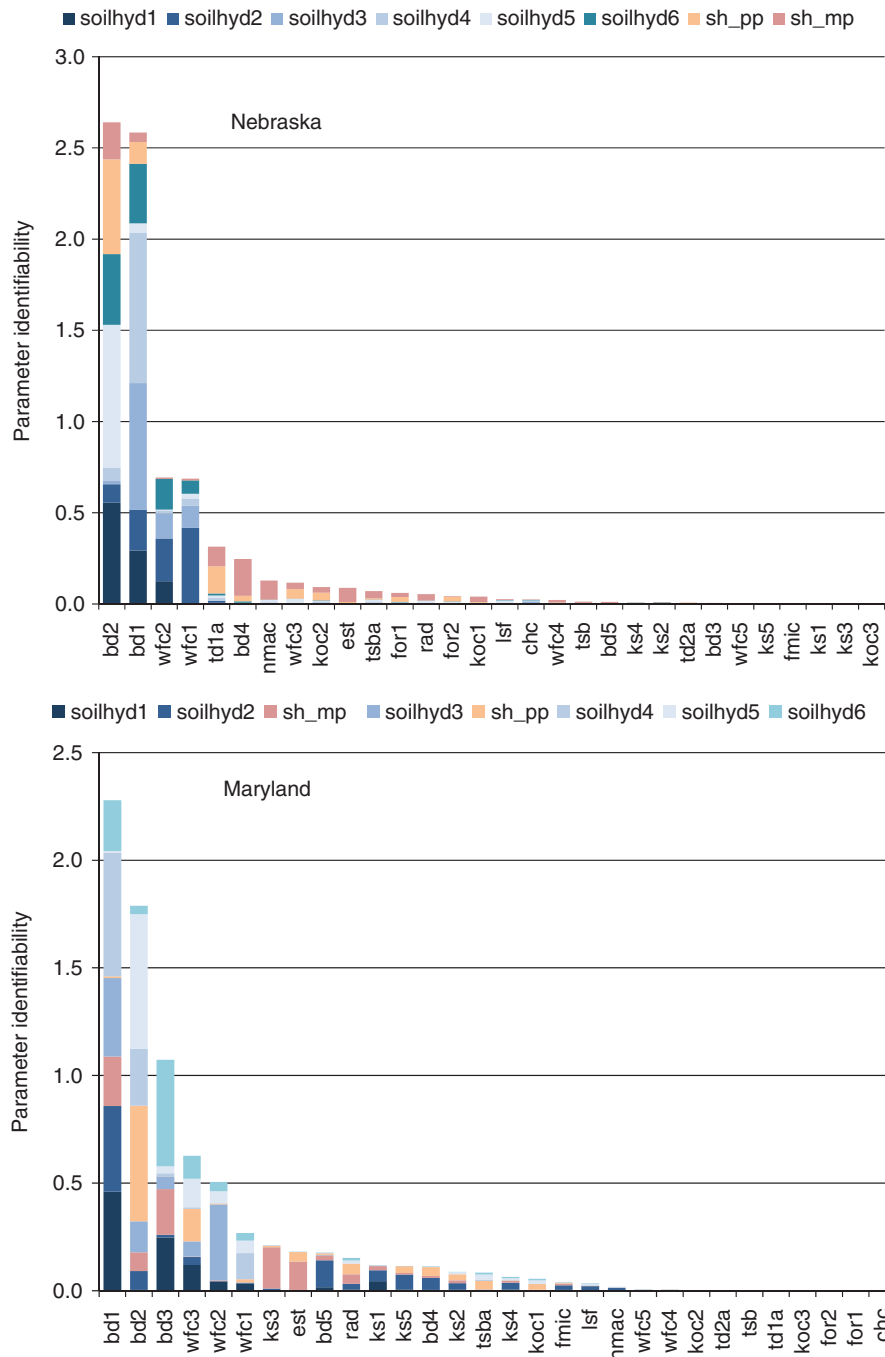


Figure 5. Parameter identifiability statistics obtained by singular value decomposition in Nebraska and Maryland. Parameters are defined in Table 3.

and MD may be attributed to differences in the organic carbon content of the soil (f_{oc}). Based on field observations of organic matter (supporting information Table S2), the weighted average f_{oc} was estimated to be 0.02 at NE and 0.009 at MD. Partition coefficients (K_d in supporting information Table S3) computed from calibrated K_{oc} values and the f_{oc} estimates were similar at NE and MD for metolachlor (4.1 and 3.2 $\text{cm}^3 \text{g}^{-1}$ respectively) and OXA (0.3 and 0.2 $\text{cm}^3 \text{g}^{-1}$ respectively), but less so for ESA (1.6 and 0.2 $\text{cm}^3 \text{g}^{-1}$ respectively).

Average measured K_d values of metolachlor and OXA for soil samples obtained from the Nashua, Iowa, field site were 3.8 and 0.9 $\text{cm}^3 \text{g}^{-1}$ respectively (supporting information Table S3). These

values were similar to those computed above for the two compounds, which supports the calibrated K_{oc} values upon which the K_d computations were based. Measured K_d values for ESA were unavailable.

3.3 Model sensitivity and prediction uncertainty

3.3.1 Sensitivity of model parameters

Identifiability (ID) was used to indicate the extent to which parameters were informed by the observed data, and parameter importance (PI) to measure the contributions of parameters to the uncertainty of maximum predicted metolachlor or degradate concentration. Whereas ID reflects all observations at all sampling

Table 4. The top ten observations informing superparameters (SPs) estimated by singular value decomposition, where the observations have been sorted by strength of activity on the SPs (activ., activity; obs., observation)

Nebraska ^a						Maryland ^b					
SP3: soil hydraulic		SP7: soil hydraulic + pesticide property		SP8: soil hydraulic + macropore		SP1: soil hydraulic		SP3: soil hydraulic + macropore		SP5: soil hydraulic + pesticide property	
Obs.	Activ.	Obs.	Activ.	Obs.	Activ.	Obs.	Activ.	Obs.	Activ.	Obs.	Activ.
mta8	0.451	ea10	0.257	mta7	0.408	ta46	0.530	mc2	0.569	md15	0.374
mta9	0.305	na17	0.226	mta6	0.303	ta47	0.479	md15	0.524	mc17	0.346
mta10	0.251	na7	0.211	mta3	0.274	ta45	0.388	md20	0.346	mc2	0.324
na4	0.215	ea12	0.207	mta4	0.238	md15	0.374	mc17	0.306	mta1	0.319
na5	0.210	na14	0.193	mta5	0.225	mc17	0.291	mta1	0.165	md12	0.270
na3	0.194	na6	0.179	mta2	0.200	mb37	0.131	mb2	0.155	mb11	0.258
na2	0.190	na13	0.170	mtb8	0.164	mb45	0.093	ta46	0.140	md20	0.249
na6	0.190	oa6	0.168	mtb6	0.164	md20	0.084	ta45	0.123	mta2	0.153
mta7	0.172	oa5	0.156	oa12	0.161	tb46	0.079	ta47	0.109	ta45	0.146
mtb7	0.171	oa7	0.152	oa11	0.151	mb2	0.060	mc20	0.092	md36	0.141

^a Nebraska: e = metolachlor ethane sulfonic acid, mt = metolachlor, n = nitrate, o = metolachlor oxanilic acid; lysimeter depth: a = 1.5 m, b = 7.0 m; number is *n*th observation at sampling point.

^b Maryland: m = moisture; n = nitrate, mt = metolachlor; t = tension; moisture probe depth: a = 0.5 m, b = 0.8 m, c = 1.1 m, d = 1.4 m; tension probe depth: a = 0.4 m, b = 1.1 m, c = 2.3 m, d = 4.1 m; lysimeter depth: a = 0.5 m; number is *n*th observation at sampling point.

depths, PI corresponds to a single prediction at the shallowest lysimeter at each field site (1.5 m at NE and 0.5 m at MD).

Soil hydraulic parameters were better informed by the observed data than pesticide properties or macropore parameters, based on ID. Bulk density parameters (bd1 and bd2) were most sensitive at both NE and MD, and bulk density and water content at field capacity (wfc) composed the four most sensitive parameters at NE and the six most sensitive at MD (Fig. 5). Soil hydraulic data were not collected at NE, but the model fit to nitrate data at NE (IA = 0.52) was about the same as at MD (IA = 0.49). $\delta^{15}\text{N}[\text{NO}_3^-]$ and $\delta^{18}\text{O}[\text{NO}_3^-]$ data were similar for shallow and deep lysimeters at a previously investigated site (N22)³⁴ that is adjacent to N23. The fact that the isotope data were similar at the two depths indicated that denitrification, which typically causes fractionation of stable isotopes, was not occurring and that nitrate was conservatively transported through the unsaturated zone. Most soil layers at NE had a moderate to high sand content (0.40–0.94) (supporting information Table S1), which is not conducive to denitrification. Nitrate evidently functioned as a conservative tracer at these sites and would be expected to move at the same rate as the soil water.

The sensitivity results reflected the observation data worth determined by SUPOBSPAR1. Soil hydraulic parameters, in particular bd and wfc, were most active on the SPs at both sites, whereas pesticide properties and macropore parameters had less overall influence. The SPs were designated on the basis of these activities as 'soil hydraulic' (soilhyd), 'soil hydraulic + pesticide properties' (sh_pp) or 'soil hydraulic + macropores' (sh_mp), as appropriate, and the colors of the bars in Fig. 5 indicate SP composition. For example, the blue colors (soilhyd) in Fig. 5 dominate the highly sensitive soil hydraulic parameters, whereas the light-orange (sh_pp) and light-red (sh_mp) shades generally correspond to less sensitive parameters.

3.3.2 Observation data worth to singular value decomposition parameters

Activities of SO elements revealed which individual observations most informed the corresponding superparameters. The top ten

most active observations are shown in sorted order in Table 4 for selected SPs to illustrate the flow of information from SOs to SPs. At NE, SP3 represented soil hydraulic processes, and the top-ranked observations were predominantly metolachlor and nitrate from the 1.5 m lysimeter. Nitrate was also active on SP7, along with ESA and OXA observations at 1.5 m depth. The increased activity of degradate observations makes sense because SP7 represents both soil hydraulic and pesticide processes. Additionally, association of nitrate with soil hydraulic processes (SP3 and SP7) corroborates the conservative transport of nitrate at these sites, which was noted above. SP8, representing soil hydraulic and macropore processes, was most informed by metolachlor observations, two of which were from the 7.0 m lysimeter. Macropores in RZWQM were parameterized so as to penetrate the entire soil profile, so it is reasonable that deep pesticide concentrations would be highly active on SP8. Also, rapid onset of observed metolachlor at 7.0 m in May 2004 is evident in Fig. 2.

At MD, SP1 – representing soil hydraulic processes – was most informed by soil water tension at 0.4 m and soil moisture observations at 0.8–1.4 m (Table 4). When soil hydraulic data were available, as at MD, they dominated soilhyd superparameters. Metolachlor appears in the top ten only for SP3 (representing soil hydraulic and macropore processes) and SP5 (soil hydraulic and pesticide properties). Although ESA and OXA observations do not appear in the top ten of any of the SPs at MD, their formation is tied to the disappearance of metolachlor in RZWQM via metolachlor half-lives and degradate formation percentages.

3.3.3 Parameter contributions to changes in prediction uncertainty

The PI statistics indicated which parameters substantially contributed to the prediction uncertainty of maximum pesticide/degradate concentration before and after calibration to the data. Precalibration prediction uncertainty was reduced by up to 46% (corresponding to wfc2) (see Fig. 6) at NE when perfect knowledge of parameters was assumed, and by up to 23% at MD (corresponding to wfc3) (Fig. 7). At both sites, the observed data caused the parameter contributions to postcalibration prediction

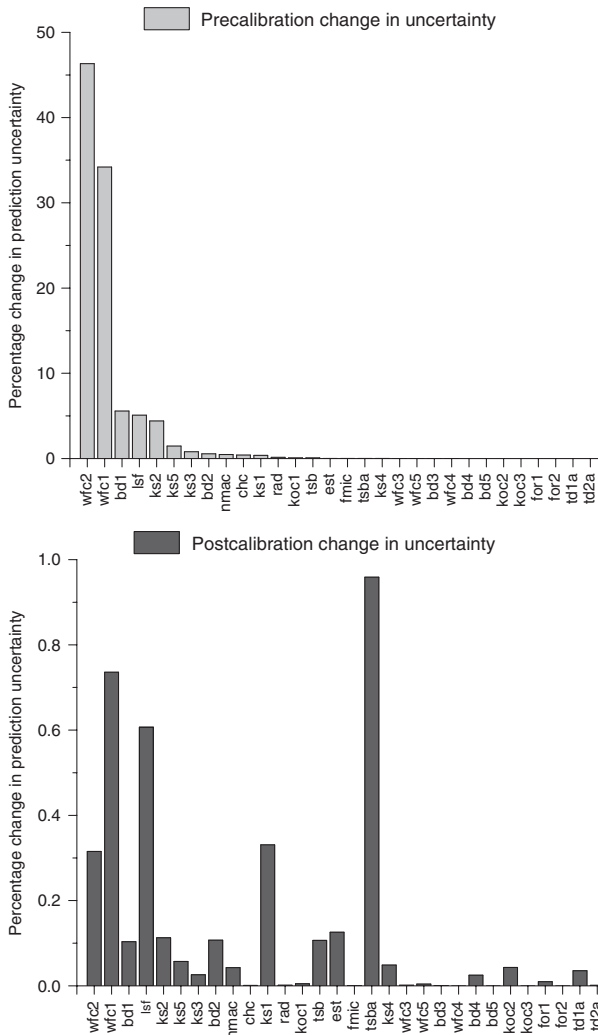


Figure 6. Contributions of parameters to pre- and postcalibration prediction uncertainties of maximum metolachlor concentration in Nebraska (0.007 mg L^{-1} at 152 cm on 29 May 2004). Parameters are defined in Table 3.

uncertainty to be small, which is seen by comparing the pre- and postcalibration PI values at NE and MD (Figs 6 and 7 respectively). The smaller the posterior uncertainty, the closer the PI values are to zero. If posterior uncertainty were zero, then assuming perfect knowledge of a parameter would result in $PI=0$ because the prediction uncertainty cannot be further reduced. Therefore, the following discussion emphasizes *relative* differences among the parameter contributions in a postcalibration context. Improved characterization of parameters with higher postcalibration PI values would be required further to reduce model misfit and prediction uncertainty beyond that which has already been achieved.

Pesticide parameters generally were more important than soil hydraulic and macropore parameters after calibration to the observed data. Half-life parameters had the highest postcalibration PI values at both sites. At NE, soil subsurface aerobic half-life of metolachlor (tsba) was the dominant parameter (black bars in Fig. 6), and at MD the dominant parameter was soil subsurface aerobic half-life of ESA (td1a), followed by soil surface biotic half-life of metolachlor (tsb) (Fig. 7). Along with sorption parameters, degradation parameters have been observed as sensitive in previous models of unsaturated zone pesticide fate and transport.^{35,36}

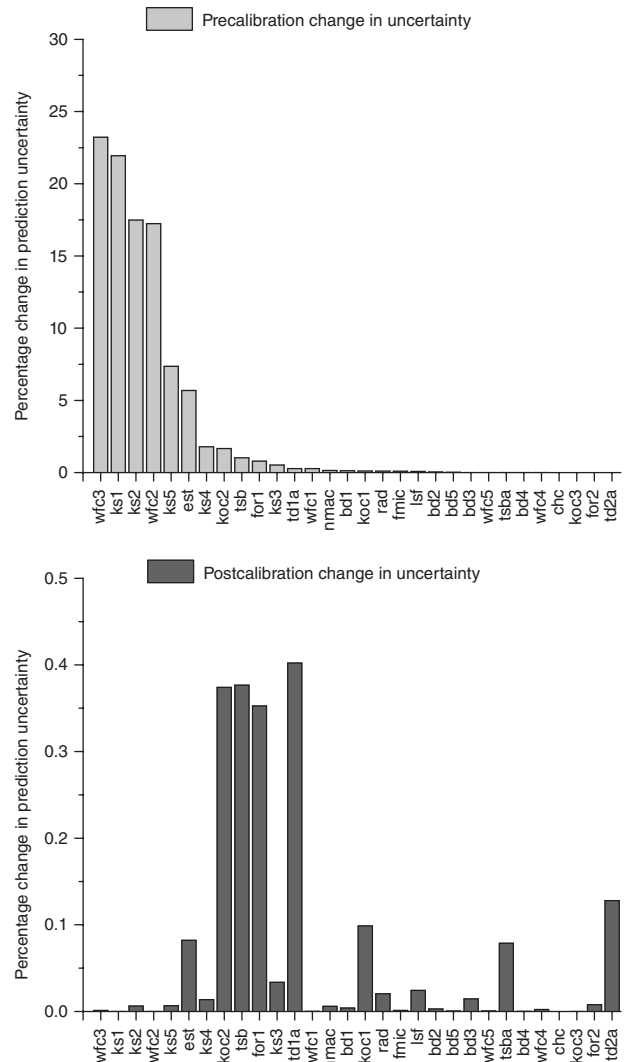


Figure 7. Contributions of parameters to pre- and postcalibration prediction uncertainties of maximum metolachlor ethane sulfonic acid concentration in Maryland (0.0041 mg L^{-1} at 52 cm on 12 January 2003). Parameters are defined in Table 3.

The lsf parameter (sorptivity factor control for lateral infiltration) was the third most important postcalibration parameter for prediction of maximum metolachlor concentration at NE (Fig. 6). This parameter controls the degree to which macropore flow is absorbed by the soil matrix via Green–Ampt radial (lateral) infiltration.² Compaction or lining of macropore walls may reduce movement of water and chemicals into the surrounding soil. In combination with tsba, these parameters suggested that transport of a less persistent pesticide to depth is enhanced when macropore flow is not diverted laterally into the soil matrix. The calibrated lsf value at NE was comparatively low (0.002 cm compared with 0.048 cm at MD), and the tsba of metolachlor was 7.6 days.

At NE, est (effective soil thickness) and nmac (number of macropores per unit area) were more important among the remaining macropore parameters. Although such parameters are seldom measured in the field, improved characterization would further reduce prediction uncertainty. Malone *et al.*¹⁸ measured nmac using tension infiltrometer data in Iowa, which resulted in accurate RZWQM predictions of herbicide concentrations in percolate. Their measured values ranged from 0.001 to 0.046 cm^{-2} at

15–35 cm depth, which brackets the present model calibrated values ($n_{mac} = 0.03 \text{ cm}^{-2}$ at both NE and MD).

Among macropore parameters at MD, est and Isf were more important than n_{mac} and rad (average macropore radius) in a postcalibration context. However, the PI value of Isf at NE was 25 times greater than that at MD, suggesting that macropore processes were less influential overall at MD. Therefore, NE would most benefit from modeling resources aimed at improving characterization of such parameters, and calibration results suggested that macropores were more active at NE than MD. The calibrated active macroporosity (p_{mac}) was about twice as high at NE (2.1×10^{-4}) than at MD (1.1×10^{-4}). This is consistent with a previous study that reported focused recharge of water in topographically low-lying areas near the NE site.¹⁴ In contrast, high vertical nitrate fluxes at MD were attributed more to the high sand content of the soils.³⁴

In general, calibrated macropore parameters obtained here were consistent with flow through former plant root channels rather than large openings typical of structured clay soils. Based on calibrated rad values (Table 3), the average macropore diameter was 0.98 mm at MD and 1.26 mm at NE, which is within the range reported for maize and alfalfa (0.4–4.5 mm) in a comprehensive review of studies on macropore flow.³⁷ In one such study, most macropores were <1 mm diameter and thought to be channels resulting from decayed plant roots. Researchers observed interconnected networks of macropores that resembled living root systems and that penetrated to >1 m depth in loess soils.

3.3.4 Observation data worth and changes in prediction uncertainty

Calibration to the available data reduced the total precalibration prediction uncertainty associated with maximum pesticide/degradate concentrations by 98.0% at NE and 98.6% at MD, based on PREDUNC1 results. Analysis of observation data worth with PREDUNC5 indicated the comparative influence of observation groups on prediction uncertainty. Values of data worth at NE indicated that metolachlor, ESA and OXA data, entered as groups one at a time, were comparable in reducing the precalibration prediction uncertainty of maximum metolachlor concentration (82–90 %) (see the gray bars in Fig. 8).

Similarly to the parameter contributions discussed above, the observed data caused a large decrease in the effect of data groups on prediction uncertainty, which is seen by comparing the pre- and postcalibration percentage changes in Fig. 8. Removal of data groups from the calibration dataset resulted in only small increases in the postcalibration uncertainty values (the black bars in Fig. 8), and the following emphasizes relative differences among data groups. None of the data groups at NE contained information so unique that their removal caused large changes in postcalibration prediction uncertainty; however, to the extent that differences were observed, metolachlor data saw the biggest increase (3.5%), which is consistent with the precalibration result. Increases incurred by removal of ESA and nitrate data were comparable (0.9 and 0.8% respectively). After metolachlor, it makes sense that ESA data were important because metolachlor disappearance and degradate formation are directly related in RZWQM, as mentioned above. At NE, nitrate data may have had moderate influence because it is conservatively transported with the soil water, which is consistent with the activity of nitrate observations on soil hydraulic SPs, noted above. Nitrate evidently functioned as a surrogate for soil water content and soil water tension data in

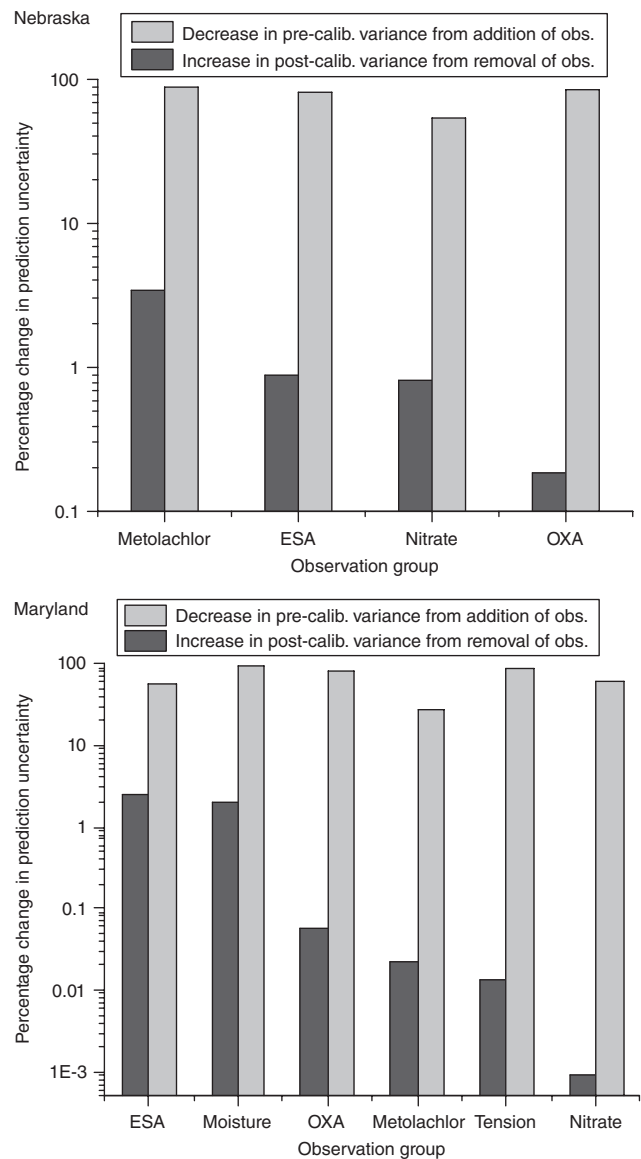


Figure 8. Data worth of observation groups to prediction of maximum metolachlor concentration in Nebraska and maximum metolachlor ethane sulfonic acid concentration in Maryland.

these well-drained soils when such data were not collected. This result underscores the utility of the multi-objective optimization approach, which simultaneously considered water and chemical data. Prior researchers have noted that data diversity, including unconventional data types, were important to convergence of parameter estimates and also helped to resolve modeling objectives with well-constrained parameters.³⁸

At MD, moisture data caused the biggest decrease in precalibration uncertainty of maximum ESA concentration (96%), followed by soil water tension (88%) and OXA data (80%) (gray bars in Fig. 8). Surprisingly, ESA data reduced this uncertainty by only 59%. However, the amount of metolachlor transformed to OXA would affect that which is transformed to ESA.

As at NE, changes in prediction uncertainty were smaller after model calibration (black bars in Fig. 8). Removal of ESA data caused the largest increase in postcalibration prediction uncertainty (2.4%), followed by moisture data (2.0%). The results suggested that collecting additional ESA data would have the

largest impact on reducing model misfit and prediction uncertainty beyond that attained so far. In contrast to NE, the increase in prediction uncertainty from removal of nitrate data was negligible (<0.01%) (Fig. 8). At MD the nitrate observations likely were redundant because soil hydraulic data were available, so there would be little point in collecting additional nitrate data.

3.3.5 Prediction intervals for water flux

Postcalibration prediction intervals of deep seepage were compared with independent estimates of groundwater recharge by the water table fluctuation method or the chloride mass balance method³⁴ to evaluate the water flux component of the models. At NE, the 95% prediction interval for deep seepage (3.9–20.9 cm year⁻¹) encompassed the independent recharge estimate (16 cm year⁻¹), which reflects irrigation. The irrigation estimate in Table 1 was obtained by water balance calculations.³⁴ At MD, the range of recharge estimates (31.5–43.4 cm year⁻¹) did not overlap with the 95% prediction interval of deep seepage (61.3–64.4 cm year⁻¹). This discrepancy suggests overestimation of deep seepage by RZWQM; however, here macropore flow was simulated at a single location in a field. The independent recharge estimates integrated water fluxes over a larger area, which may have dampened preferential flow effects at any one location.

4 CONCLUSIONS

The following conclusions were drawn from this research:

- 1 Calibration of complex agricultural system models is essential, but collection of unsaturated zone data is time consuming and expensive. Study results indicated which data observations most benefitted the modeling. Although the observed data were comparatively sparse, they substantially reduced the prediction uncertainty associated with maximum pesticide/degradate concentrations in unsampled portions of breakthrough curves.
- 2 Nitrate functioned as a conservative unsaturated zone tracer and evidently was a surrogate for soil hydraulic data at NE. Nitrate observations at NE tended to dominate superparameters that reflected soil hydraulic processes. Even though soil hydraulic data were not available for model calibration at NE, the independently measured recharge estimate (16 cm year⁻¹) was well within the 95% prediction interval for deep seepage (3.9–20.9 cm year⁻¹).
- 3 In contrast, nitrate data were somewhat redundant to predicting maximum ESA concentration when soil hydraulic data were collected, as at MD. Soil moisture and soil water tension dominated superparameters at this site. Whereas moisture data at MD caused the largest decrease in precalibration prediction uncertainty, nitrate data caused the fourth-largest decrease.
- 4 Soil hydraulic parameters were more sensitive and better informed by the observed data at both sites, and pesticide and macropore properties were more important to prediction uncertainty that remained after model calibration. Better characterization of the latter parameters would be required further to reduce model misfit and prediction uncertainty.
- 5 Macropore parameters tended to be more important at NE than at MD, which was seen by comparing parameter contributions to postcalibration prediction uncertainty at the two sites. Calibrated macropore parameters at both sites generally were

consistent with flow through former plant root channels rather than large openings.

ACKNOWLEDGEMENTS

The authors wish to thank the field personnel who collected the data used in this study. They also thank Mike Fienen, Claire Tiedeman and two anonymous reviewers for insightful reviews of the draft manuscript.

SUPPORTING INFORMATION

Supporting information may be found in the online version of this article.

REFERENCES

- 1 Gilliom RJ, Barbash JE, Crawford CG, Hamilton PA, Martin JD, Nakagaki N *et al.*, The quality of our nation's waters – pesticides in the nation's streams and ground water, 1992–2001. US Geological Survey Circular 1291, Reston, VA, 172 pp. (2006).
- 2 Ahuja LR, Rojas KW, Hanson JD, Shaffer MJ and Ma L, *Root Zone Water Quality Model – Modelling Management Effects on Water Quality and Crop Production*. Water Resources Publications LLC, Highlands Ranch, CO (2000).
- 3 Nolan BT, Puckett LJ, Ma L, Green CT, Bayless ER and Malone RW, Predicting unsaturated zone nitrogen mass balances in agricultural settings of the United States. *J Environ Qual* **39**(3):1051–1065 (2010).
- 4 Beven K, *Rainfall-Runoff Modelling: the Primer*. John Wiley & Sons, Ltd, Chichester, UK (2001).
- 5 Aster RC, Borchers B and Thurber C, *Parameter Estimation and Inverse Problems*. Elsevier Academic Press, Amsterdam, The Netherlands (2005).
- 6 Doherty J and Hunt RJ, Two statistics for evaluating parameter identifiability and error reduction. *J Hydrol* **366**(1–4):119–127 (2009).
- 7 Hill MC and Tiedeman CR, *Effective Groundwater Model Calibration With Analysis of Data, Sensitivities, Predictions, and Uncertainty*. John Wiley & Sons, Inc., Hoboken, NJ (2007).
- 8 Tonkin MJ and Doherty J, A hybrid regularized inversion methodology for highly parameterized environmental models. *Water Resour Res* **41**(W10412):1–16 (2005).
- 9 Doherty J and Welter D, A short explanation of structural noise. *Water Resour Res* **46**(W05525):1–14 (2010).
- 10 Lu D, Ye M and Hill MC, Analysis of regression confidence intervals and Bayesian credible intervals for uncertainty quantification. *Water Resour Res* **48**(W09521):1–20 (2012).
- 11 Dausman AM, Doherty J, Langevin CD and Sukop MC, Quantifying data worth toward reducing predictive uncertainty. *Groundwater* **48**(5):729–740 (2010).
- 12 Bayless ER, Capel PD, Barbash JE, Webb RMT, Hancock TLC and Lampe DC, Simulated fate and transport of metolachlor in the unsaturated zone, Maryland, USA. *J Environ Qual* **37**(3):1064–1072 (2008).
- 13 Capel PD, McCarthy KA and Barbash JE, National, holistic, watershed-scale approach to understand the sources, transport, and fate of agricultural chemicals. *J Environ Qual* **37**(3):983–993 (2008).
- 14 Hancock TC, Sandstrom MW, Vogel JR, Webb RMT, Bayless ER and Barbash JE, Pesticide fate and transport throughout unsaturated zones in five agricultural settings, USA. *J Environ Qual* **37**(3):1086–1100 (2008).
- 15 Ma L, Malone RW, Heilman P, Karlen DL, Kanwar RS, Cambardella CA *et al.*, RZWQM simulation of long-term crop production, water and nitrogen balances in Northeast Iowa. *Geoderma* **140**(3):247–259 (2007).
- 16 Ma L, Ahuja LR, Nolan BT, Malone RW, Trout TJ and Qi Z, Root Zone Water Quality Model (RZWQM2): model use, calibration, and validation. *Trans ASABE* **55**(4):1425–1446 (2012).
- 17 Malone RW, Ahuja LR, Ma L, Wauchope RD, Ma Q and Rojas KW, Application of the Root Zone Water Quality Model (RZWQM) to pesticide fate and transport: an overview. *Pest Manag Sci* **60**(3):205–221 (2004).

- 18 Malone RW, Logsdon S, Shipitalo MJ, Rice JW, Ahuja L and Ma L, Tillage effect on macroporosity and herbicide transport in percolate. *Geoderma* **116**(1–2):191–215 (2003).
- 19 Malone RW, Ma L, Wauchope RD, Ahuja LR, Rojas KW, Ma Q *et al.*, Modeling hydrology, metribuzin degradation and metribuzin transport in macroporous tilled and no-till silt loam soil using RZWQM. *Pest Manag Sci* **60**(3):253–266 (2004).
- 20 Doherty J. *PEST – Model Independent Parameter Estimation*. Watermark Numerical Computing, Brisbane, Australia (2010).
- 21 Houska T, Multsch S, Kraft P, Frede H-G, and Breuer L, Monte Carlo-based calibration and uncertainty analysis of a coupled plant growth and hydrological model. *Biogeosciences* **11**:2069–2082 (2014).
- 22 Raat KJ, Vrugt JA, Bouten W and Tietema A, Towards reduced uncertainty in catchment nitrogen modelling: quantifying the effect of field observation uncertainty on model calibration. *Hydrol Earth Syst Sci* **8**(4):751–763 (2004).
- 23 Fienen MN, Muffels CT and Hunt RJ, On constraining pilot point calibration with regularization in PEST. *Groundwater* **47**(6):835–844 (2009).
- 24 Fienen MN, Doherty JE, Hunt RJ and Reeves HW, Using prediction uncertainty analysis to design hydrologic monitoring networks: example applications from the Great Lakes water availability pilot project. US Geological Survey Scientific Investigations Report 2010-5159, Reston, VA, 44 pp. (2010).
- 25 Doherty J, *Addendum to the PEST Manual*. Watermark Numerical Computing, Brisbane, Australia (2013).
- 26 Legates DR and McCabe GJ, Evaluating the use of ‘goodness-of-fit’ measures in hydrologic and hydroclimatic model evaluation. *Water Resour Res* **35**(1):233–241 (1999).
- 27 Meyer PD, Rockhold ML and Gee GW, Uncertainty analyses of infiltration and subsurface flow and transport for SDMP sites. US Nuclear Regulatory Commission Report NUREG/CR-6565, Washington, DC, 38 pp. (1997).
- 28 Doherty JE, Hunt RJ and Tonkin MJ, Approaches to highly parameterized inversion: a guide to using PEST for model-parameter and predictive-uncertainty analysis. US Geological Survey Scientific Investigations Report 2010-5211, Reston, VA, 71 pp. (2010).
- 29 Malone RW, Nolan BT, Ma L, Kanwar RS, Pederson C and Heilman P, Effects of tillage and application rate on atrazine transport to subsurface drainage: evaluation of RZWQM using a six-year field study. *Agric Water Manag* **132**(January):10–22 (2014).
- 30 Groschen GE, Arnold TL, Harris MA, Dupre DH, Fitzpatrick FA, Scudder BC *et al.*, Water quality in the Upper Illinois River Basin, Illinois, Indiana, and Wisconsin, 1999–2001. US Geological Survey Circular 1230, Reston, VA, 32 pp. (2004).
- 31 Kalkhoff SJ, Kolpin DW, Thurman EM, Ferrer I and Barcelo D, Degradation of chloroacetanilide herbicides: the prevalence of sulfonic and oxanilic acid metabolites in Iowa groundwaters and surface waters. *Environ Sci Technol* **32**(11):1738–1740 (1998).
- 32 Mills PC, Kolpin DW, Scribner EA and Thurman EM, Herbicides and degradates in shallow aquifers of Illinois: spatial and temporal trends. *J Am Water Resour Ass* **41**(3):537–547 (2005).
- 33 Kalkhoff SJ, Lee KE, Porter SD, Terrio PJ and Thurman EM, Herbicides and herbicide degradation products in upper midwest agricultural streams during August base-flow conditions. *J Environ Qual* **32**(3):1025–1035 (2003).
- 34 Green CT, Fisher LH and Bekins BA, Nitrogen fluxes through unsaturated zones in five agricultural settings across the United States. *J Environ Qual* **37**(3):1073–1085 (2008).
- 35 Dubus IG and Brown CD, Sensitivity and first-step uncertainty analyses for the preferential flow model MACRO. *J Environ Qual* **31**:227–240 (2002).
- 36 Close ME, Lee R, Sarmah AK, Pang L, Dann R, Magesan GN *et al.*, Pesticide sorption and degradation characteristics in New Zealand soils – a synthesis from seven field trials. *NZ J Crop Hort Sci* **36**(1):9–30 (2008).
- 37 Jarvis NJ, Review of non-equilibrium water flow and solute transport in soil macropores: principles, controlling factors and consequences for water quality. *Eur J Soil Sci* **58**(3):523–546 (2007).
- 38 Hunt RJ, Feinstein DT, Pint CD and Anderson MP, The importance of diverse data types to calibrate a watershed model of the Trout Lake Basin, Northern Wisconsin, USA. *J Hydrol* **321**(1–4):286–296 (2006).